Optimal Design of a Packed Bed Reactor with Turner's Mixing Model

Optimal Design of a Packed Bed Reactor
with Turner's Mixing Model

Kenji Kubo*, Daisaburo Kato*

ABSTRACT

Optimum temperature profiles were computed along the axial direction of a packed bed flow reactor, by utilizing two types of simplified Turner's side pocket models for the description of non-ideal mixing characteristics. Comparison is also made with the profile when Taylor's diffusion model is cited.

The finding is that, for large variance of residence time distribution, i.e. for shallow bed condition, the optimal temperature profile calculated with simplified Turner's models is higher at near after the entrance of the reactor and lower at near before the exit than that with Taylor's model. By operating a reactor according to the optimum temperature profile with the Turner's models, the length of the reactor can be greatly reduced.

Key Words: Optimal design of reactor, Optimal temperature profile, Fluid mixing, Side pocket model

Introduction

In designing a thermal reactor packed with catalyst, exact knowledge of the optimum temperature profile is important to operate the reactor at its maximum yield. Many papers have dealt with the problem of the optimum temperature profile along its axial direction. Some are based on the assumption of piston flow[3,4,19-24,26], some are on the basis of CSTR[9,28,30], and the others are of Taylor's apparent diffusion (dispersion) model[9,16,18,25,26] as an axial mixing model. They show that the optimum temperature profile along the axial direction of the reactor is affected by the non-ideal mixing characteristics.

According to the results of dynamic model identification[12,14], of flowpattern observation[1,15] and of measurement of residence time distribution[2,13] in packed beds, the side pocket type models[7,14,28] can describe the non-ideal mixing characteristics more exactly than Taylor's diffusion model, especially in a transition flow region for shallow bed condition. In the present study, computation of optimum temperature profile has been executed by employing Turner's side pocket models in describing the non-ideal
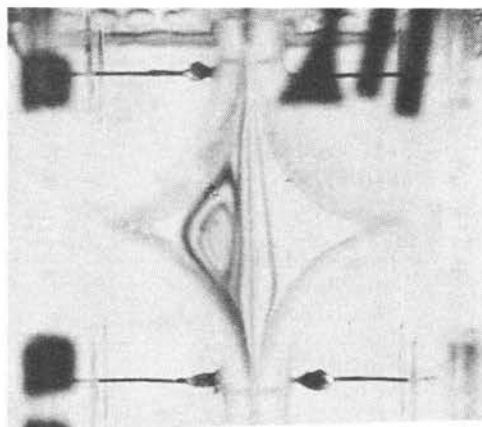

Figure 1 Flow pattern in transition region at a void of a tube bundle bed.

fluid mixing. Computation with Taylor's apparent diffusion (or dispersion) model is also done. Discussion was made by comparing the both results with the same kinetic data.

Simplified Turner's Models

Figure 1 shows a typical example of flow pattern in a transition region observed in a void of a tube bundle bed as a two dimensional model of packed bed. At the center of the void, the fluid is very rapidly flowing and seems to be in piston flow. The fluid at both sides of the void space is observed to be in rotating flow. From these facts and another observations[1,2,12,13,15] it has been decided to describe the characteristics in packed beds in laminar and transition regions by two types of macro-axial mixing models after Turner[28] as follows.

1) Distributed side mixing model (DSM model)

DSM model is intended to simulate the behavior of flow pattern in a transition region. Main flow at the center of the void is assumed to be in piston flow, and side flow part, corresponding to rotating fluid in the side pocket part of the void, is taken as distributed perfect mixing cells along the bed after Cholette and Cloutier[7]. There exists a resistance to mixing between the two parts.

2) Distributed side diffusion model (DSD model)

In this model it is assumed that the main flow part is in piston flow and the side flow part has only side diffusion, but no axial diffusion.

Schematic illustrations, governing equations and boundary conditions of these two models are shown in **Table 1**. These models are modified versions of Turner's side pocket model[28] and have two parameters; volume fraction, β, and side

Table 1

Simplified Turner's models, having distributed side pocket

MODEL	DISTRIBUTED SIDE MIXING MODEL (DSM)	DISTRIBUTED SIDE DIFFUSION MODEL (DSD)
GOVERNING EQUATION	$u_x \dfrac{\partial F_1}{\partial x} - \dfrac{1}{R_M}(F_2 - F_1)$ $\qquad - (1-\beta)R_1 = 0 \quad (1)$ $\dfrac{1}{R_M}(F_1 - F_2) + \beta R_2 = 0 \quad (2)$	$u_x \dfrac{\partial F_1}{\partial x} + \dfrac{E_y}{L_x}\left(\dfrac{\partial F_2}{\partial y}\right)_{y=L_y}$ $\qquad - (1-\beta)R_1 = 0 \quad (3)$ $E_y \dfrac{\partial^2 F_2}{\partial y^2} + \beta R_2 = 0 \qquad (4)$
BOUNDARY CONDITION	$F_1 = 0 \qquad (\text{at } x=0)$	$\left(\dfrac{\partial F_2}{\partial y}\right)_{y=0} = 0 \quad \begin{array}{l} F_2 = F_1 \ (\text{at } y=L_y) \\ F_1 = 0 \ (\text{at } x=0) \end{array}$
ILLUSTRATION		
MEAN VARIANCE 3RD MOMENT	$\bar{\tau} = 1.0$ $\overline{\tau^2} = 2\beta^2/M$ $\overline{\tau^3} = 6\beta^3/M^2$	$\bar{\tau} = 1.0$ $\overline{\tau^2} = (2/3)\beta^2 Pe_y$ $\overline{\tau^3} = (4/5)\beta^3 Pe_y^2$

mixing factor, M, for the DSM model, and β and side mixing Peclet number, Pe_y, for the DSD model, while the Taylor's diffusion model has only one parameter; axial mixing Peclet number, Pe. These parameters (β and M, or β and Pe_y) can be evaluated from the variance and the third moment ($\overline{\tau^2}$, $\overline{\tau^3}$) of experimental residence time distribution, since $\overline{\tau^2}$, $\overline{\tau^3}$ of each model are derived and listed in Table 1.

Computation of Optimum Temperature profile

1) DSD model A first order reversible reaction $A \underset{k_B}{\overset{k_A}{\rightleftharpoons}} B$ is employed as a model reaction. It is desired to maximize the yield of the B component at the reactor outlet ($\xi = 1.0$) by adjusting the temperature profile along the reactor. Let the pure A be fed to the reactor inlet. The governing differential equations associated with the DSD model are given by Equations (5) and (6). Where F_1 and F_2, respectively, are the mole fractions of the component B in the main and side flow parts.

$$\frac{\partial F_1}{\partial \xi} + \frac{1}{Pe_y}\left(\frac{\partial F_2}{\partial \eta}\right)_{\eta=1}$$
$$- (1-\beta)\left(\frac{L_x}{u_x}\right)[k_A(1-F_1) - k_B F_1] = 0 \quad (5)$$

$$\frac{1}{Pe_y}\left(\frac{\partial^2 F_2}{\partial \eta^2}\right) + \beta\left(\frac{L_x}{u_x}\right)[k_A(1-F_2) - k_B F_2]$$
$$= 0 \quad (6)$$

where k_A and k_B are the reaction rate constants, Pe_y is the side mixing Peclet number and β is the volume fraction of the side flow part. The boundary conditions are written as Equations (7), (8) and (9).

$$F_1 = 0 \quad \text{at } \xi = 0 \quad (7)$$
$$F_1 = F_2 \quad \text{at } \eta = 1 \quad (8)$$
$$\frac{\partial F_2}{\partial \eta} = 0 \quad \text{at } \eta = 0 \quad (9)$$

Equation (6) is solved with the boundary condition of Equation (9), and F_2 is given by Equation (10).

$$F_2 = F_2(0) \cosh\sqrt{(A+B)}\eta$$
$$- \frac{A}{A+B}[\cosh\sqrt{(A+B)}\eta - 1] \quad (10)$$

where $A = \beta(L_x/u_x)Pe_y k_A$, $B = \beta(L_x/u_x)Pe_y k_B$. By utilizing Equation (8) as the other boundary condition, Equation (10) becomes Equation (11).

$$F_2 = \frac{A}{A+B} + \frac{F_1 - A/(A+B)}{\cosh\sqrt{(A+B)}}\cosh[\sqrt{(A+B)}\eta] \quad (11)$$

Thus, substituting Equation (11) for F_2 of Equation (5), the required state equation of this process is derived as Equation (12).

$$\frac{\partial F_1}{\partial \xi} = -\left[\frac{\sqrt{A+B}}{Pe_y}\tanh\sqrt{A+B} + X(k_A + k_B)\right]F_1$$
$$+ \frac{A}{\sqrt{A+B}\,Pe_y}\tanh\sqrt{A+B} + Xk_A \quad (12)$$

where $X = (L_x/u_x)(1-\beta)$. The Hamiltonian, H, is given by Equation (13).

$$H = Z_1 \frac{\partial F_1}{\partial \xi} \quad (13)$$

and the adjoining equation is expressed by Equation (14) which can be obtained by differentiating H in Equation (13) with F_1.

$$\frac{\partial Z_1}{\partial \xi} = -\frac{\partial H}{\partial F_1} = Z_1\left[\frac{\sqrt{A+B}}{Pe_y}\tanh\sqrt{A+B}\right.$$
$$\left. + X(k_A + k_B)\right] \quad (14)$$

As the object is to maximize F_1 at outlet of the reactor, the boundary condition on Z_1 at outlet ($\xi = 1.0$) is given by Equation (15).

$$Z_1(1) = 1.0 \quad (15)$$

For simplification of mathematical handling, the temperature in main flow part is assumed to be equal to that in side flow part. The optimal operating condition is given by partial differentiation of Hamiltonian of Equation (13) with temperature, T, and by equating it to be zero. By this procedure, optimum concentration F_1 is derived as Equation (16).

$$F_1 = \left[2E_A A\sqrt{A+B} - \frac{A}{\sqrt{A+B}}(E_A A\right.$$
$$\left. + E_B B)\tanh\sqrt{A+B} + \frac{A(E_A A + E_B B)}{(A+B)\cosh^2\sqrt{A+B}}\right.$$

$$+ 2Pe_yXE_Ak_A] / [(E_AA + E_BB)(\frac{\tanh\sqrt{A+B}}{\sqrt{A+B}}$$

$$+ \frac{1}{\cosh^2\sqrt{A+B}}) + 2Pe_yX(E_Ak_A + E_Bk_B)] \tag{16}$$

Dimensionless reactor length, ξ for given T can be computed by numerical integration of Equation (17), via $\partial F_1/\partial\xi$ of Equation (12) and via $\partial F_1/\partial T$ which is given by partial differentiation of F_1 of Equation (16) with temperature, T.

$$\xi = \int_{T=T_{(\xi=0)}}^{T=T_{(\xi=1)}} \frac{\partial F_1}{\partial T} / \frac{\partial F_1}{\partial\xi} \, dT \tag{17}$$

Temperature profile along the reactor length, ξ, can be plotted from this ξ-T relation. Concentration profile, F_1-ξ, can be also computed from this ξ-T relation and Equation (16).

2) DSM model The optimum temperature and concentration profiles with the DSM model are computed in the similar manner as mentioned above with the DSD model.

The mathematical development and numerical computation for the both types of the modified Turner's models are found to be easier than those for Taylor's diffusion model.

<div align="center">

Table 2

Kinetic Data Used to Compute Figures 2 to 5

</div>

k_{A0}	2.51×10^5	h^{-1}
k_{B0}	1.995×10^7	h^{-1}
E_A	5.556×10^3	g-cal/g-mole
E_B	1.111×10^4	g-cal/g-mole
R_g	1.987	g-cal/g-mole K
L_x	304.8	cm
u_x	304.8	m/h

Computational Results and Discussion

1) DSD model **Figures 2** and 3 show the computed optimum temperature and concentration profiles. For convenience of comparison, kinetic data are adjusted to those of Fan's numerical data[9], as was listed in **Table 2**, that had been cited for computation with Taylor's model. Figure 2 shows
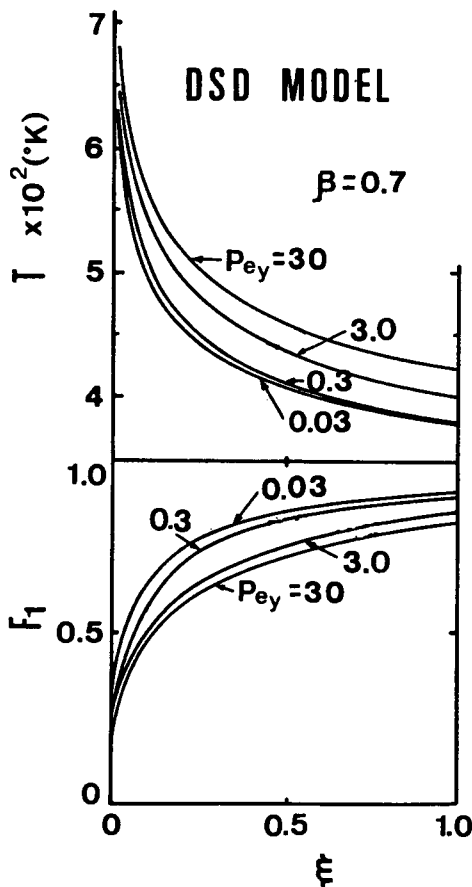

Figure 2 Optimum temperature and concentration profiles with DSD model by letting β constant at 0.7.

optimum temperature, T, for the DSD model plotted as a function of dimensionless reactor length, ξ, for Pe_y = 0.03, 0.3, 3.0 and 30.0 by letting β be constant at 0.7. The corresponding concentration profiles of substance B are also plotted in Figure 2. It has been noted that, if Pe_y is less than 0.06, the optimum temperature and concentration profiles become nearly the same as the profiles without side diffusion. It can be noted that the yield of B decreases as Pe_y increases, that is, as the side diffusion is reduced.

In the case of employing β as a variable, the profiles of temperature and concentration were also computed for constant Pe_y. According to the results, the yield of substance B increases with a decrease in β, i.e. volume fraction of side part.

When β is less than 0.1, the profiles are agreement with the profiles of piston flow condition without side diffusion within 1.0% of maximum error.

Therefore, if a higher yield is disired to be attained, the reactor should be designed so as to have smaller value of β or Pe_y by selecting a proper shape of packing or flow conditions, to reduce β; the fraction of side flow part.
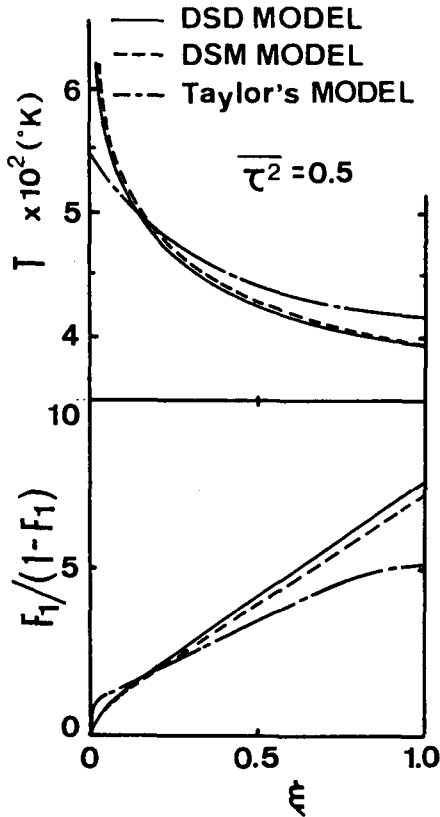

Figure 3 Comparison of optimum temperature and concentration profiles among three models under the same variance, $\overline{\tau^2} = 0.5$, Pe = 2.56, Pe_y = 3.0, M = 1.0, $\beta = 0.5$

2) DSM model The variances of the DSM model and the DSD model are $2\beta^2/M$ and $(2/3)\beta^2 Pe_y$, respectively. By equating these both variances, M is equal to $3/Pe_y$. Considering above relationship between M and Pe_y, the profiles of T and F_1 with the DSM model are similar to those with the DSD model in their shapes as shown in **Figure 4**. With value of β below 0.3, the profiles of two side pocket models show agreement with each other

within 1.0% of maximum error. As is the case with the **DSD** model, β and M are found to affect the yield of reactor, when we employ the DSM model as a non-ideal mixing model. In order to increase the yield of reactor, it is important that the reactor should be designed and operated by making β and 1/M as little as possible. Pulsation of feed flow rate may also promote the mixing in the side flow part, therefore, can decrease 1/M.

3) Comparison of profiles among two side pocket models and the diffusion model In the upper part of Figure 3, the optimum temperature profiles are compared among the **DSD**, the **DSM** and the diffusion model with an identical variance. It is shown that optimum temperature profiles with two
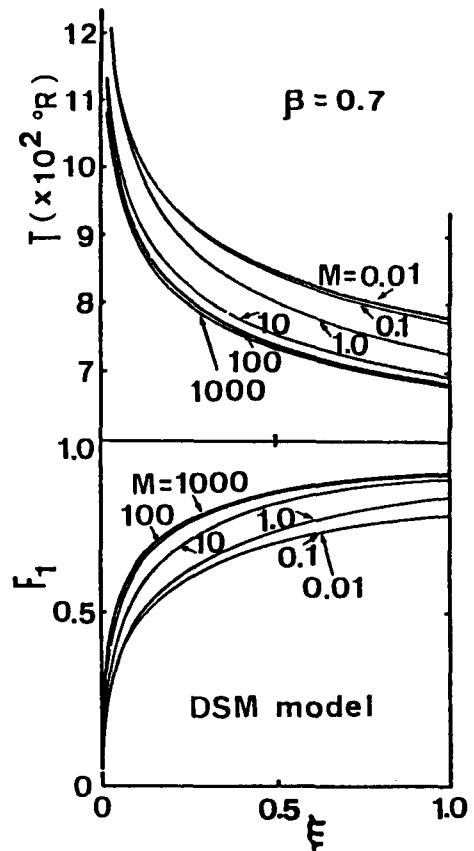

Figure 4 Optimum temperature and concentration profiles with DSM model by letting β constant at 0.7.

distributed side pocket models are rather higher at the entrance part of the reactor and lower at the outlet part than that with taylor's diffusion model. The axial concentration profiles are converted into the form of the selectivity, $F_1/(1-F_1)$, which represents F_{1B}/F_{1A}, and shown in the lower part of Figure 3. The profiles of the selectivity show clearly that a reactor which is designed and operated by the optimum profile computed with Turner's distributed side pocket models is expected to have higher selectivity for substance B than that with Taylor's diffusion model. As for a trickle bed type reactor, Turner's model is also reported to be able to describe more accurately non-ideal mixing than Taylor's diffusion model[10]. So, these optimum profiles can be applied directly the design of a trickle bed type reactor.

4) Comparison of length of reactor among two side pocket models and diffusion model Ratio of reactor length (saving fraction: ϕ) calculated with the DSD or DSM model to the length calculated with Taylor's model is plotted in **Figure 5** against the variance, when a reactor is operated according to the optimum temperature for each model with
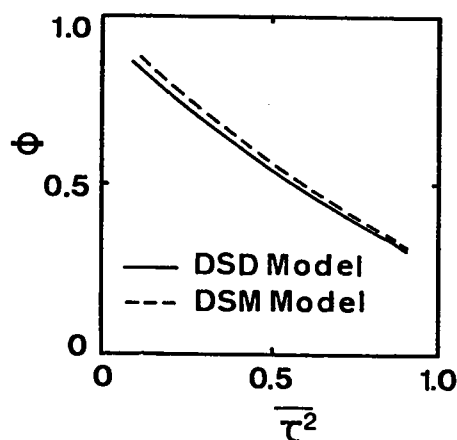
an identical variance. As the base for the computation, the length of the reactor with taylor's model is selected to be $3m$. The length of the reactor with DSD and DSM models are determined so as to give the same yield of the Taylor's reactor of $3m$. The Figure uses $\beta=0.3$, which is obtained by the experiments for long and shallow beds[12, 14]. This shows that the reactor length decreased with the increase of variance for DSD or DSM models. The length of the reactor with the side pocket models is saved nearly 50% at $\overline{\tau^2}=0.6$ and is approximately 70% at $\overline{\tau^2}=0.9$. These circumstances of large variance are found to be realized[12, 14], for example, under a transition flow for shallow bed condition. Length of a reactor can be shortened considerrably by operating a reactor according to the optimum temperature with side pocket models in comparison with the diffusion model. So, for the design and operation of a thermal reactor, the thermal policy which utilizes the side pocket models is very desirable from the viewpoint of saving the reactor length, especially in a transition flow for shallow bed condition.

Conclusion

The optimum temperature profile computed with Turner's side pocket type model is rather higher at immediately after the entrance of reactor and lower at near before the outlet than that of Taylor's model. The design or operation of a thermal reactor by utilizing the side pocket models as a non-ideal mixing model is able to bear full fruit from the viewpoint of saving the length of reactor, especially in a transition flow for shallow bed condition.

Figure 5 Saving fraction of reactor length
ϕ = (reactor length with DSD or DSM model)/
(reactor length with Taylor's model)

Nomenclature

E_A, E_B = activation energies
E_y = side diffusion coefficient

F   = dimensionless concentration of B component

H   = Hamiltonian function

k_A, k_B = rate constants

k_{A0}, k_{B0} = frequency factors

L_x = axial length of packed bed

L_y = length of side diffusion in DSD model

M   = side mixing factor ($= L_x/R_M u_x$)

Pe   = Peclet number

Pe_y = side mixing Peclet number ($= u_x L_y^2/ E_y L_x$)

R   = reaction term

R_g = gas constant

R_M = side mixing resistance

T   = temperature

u_x = interstitial linear velocity

x   = axial distance, flow direction

y   = distance normal to x, lateral to flow direction

< Greek letters >

β = volume fraction of side part in a void

ξ = dimensionless axial length, at inlet $\xi =$ 0, at outlet $\xi = 1$

η = dimensionless length of side direction

ϕ = saving fraction of reactor length [=(reactor length with the DSD or DSM model)/(reactor length with Taylor's model)]

τ = dimensionless time

$\bar{\tau}$ = mean residence time, in terms of τ

$\overline{\tau^2}$ = variance of residence time with regard to $\bar{\tau}$

$\overline{\tau^3}$ = 3rd moment

< Subscript >

1   = main flow part

2   = side flow part

References

(1) Aratani T., K. Kubo, A. Mishima and T. Yano, Journal of Chem. Eng. of Japan, 9, 334 (1976).

(2) Aratani T., K. Kubo, A. Mishima and T. Yano, Bull. Univ. Osaka Pref., 25, 37 (1976).

(3) Bernard Gillespie and James J. Carberry, Ind. Eng. Chem. Fundam., 5, 165 (1966).

(4) Binns D. T., T. A. Kantyka and R. C. Welland, Trans. Instn. Engrs., 47, T53 (1969).

(5) Chang K. S. and S. G. Bankoff, A.I.Ch.E. Journal, 15, 410 (1969).

(6) Chauhan S. P., J. P. Bell and R. J. Adler, Chem. Eng. Sci., 27, 585 (1972).

(7) Cholette A. and L. Cloutier, Can. J. Chem. Eng., 37, 105 (1959).

(8) Fan L. T., L. E. Erickson, R. W. Sucher and G. S. Mathad, Ind. Eng. Chem., Process Des. Dev., 4, 431 (1965).

(9) Fan L. T., The Continuous Maximum Principle (1966).

(10) Gavalas George R., A.I.Ch.E. Journal, 17, 787 (1971).

(11) Hoogendroom C. J. and J. Lips, Can. J. Chem. Eng., 43, 125 (1965).

(12) Kubo K., T. Aratani, A. Mishima and T. Yano, Journal of Chem. Eng. Japan, 11, 234 (1978).

(13) Kubo K., T. Aratani, A. Mishima and T. Yano, Chem. Eng. Journal, 18, 209 (1979).

(14) Kubo K., T. Aratani and A. Mishima, International Chem. Eng., 23, 85 (1983).

(15) Kubo K., T. Aratani, A. Mishima and T. Yano, Journal of Chem. Eng. of Japan, 11, 405 (1978).

(16) Lee E. Stanley, A. I. Ch. E. Journal, 10, 309 (1964).

(17) Leung Vincent P and Kun S. Chang, A. I. Ch. E. Journal, 15, 782 (1969).

(18) Lynn Leroy L., Elliot S. Parkin and Raymond L. Zahradnik, Ind. Eng. Chem. Fandam., 9, 58 (1970).

(19) Mckinstry K. A., F. J. Stermole and R. L. Dunn, A. I. Ch. E. Journal, 18, 206 (1972).

(20) Newberger Mark R. and Robert H. Kadlec, A. I. Ch. E. Journal, 17, 1381 (1971).

(21) Nishida N., A. Ichikawa and E. Tazaki, A. I. Ch. E. Journal, 18, 561 (1972).

(22) Okazaki T., M. Okuda and H. Shingu, Seigyo Kogaku, Japan, 12, 146 (1967).

(23) Paynter J. D. and S. G. Bankoff, Can. J. Chem. Eng., 44, 340 (1966).

(24) Paynter J. D. and S. G. Bankoff, Can. J.

Chem. Eng., **45**, 226 (1967).

(25) Takamatsu T., I. Hashimoto and Y. Sawanoi, Seigyo Kogaku, Japan, **13**, 469 (1967).

(26) Takamatsu T., I. Hashimoto and F. Yoshida, Seigyo Kogaku, Japan, **13**, 664 (1967).

(27) Takamatsu T., I. Hashimoto and F. Yoshida, System and Control, Japan, **17**, 113 (1973).

(28) Turner, G. A., Chem. Eng. Sci., **7**, 156 (1957).

(29) Wan Chee-Gen and Edward N. Ziegler, Ind. Eng. Chem. Fandam., **19**, 55 (1973).

(30) Weinstein H. and R. J. Adler, Chem. Eng. Sci., **22**, 65 (1967).